IOP Publishing Science and Technology of Advanced Materials
Sci. Technol. Adv. Mater. **9** (2008) 035004 (7pp) doi:10.1088/1468-6996/9/3/035004

Enhanced bioactivity of ZnO nanoparticles—an antimicrobial study

Nagarajan Padmavathy and Rajagopalan Vijayaraghavan

School of Science and Humanities—Materials Division, VIT University, Vellore – 632 014, Tamil Nadu, India

E-mail: rvijayaraghavan@vit.ac.in

Received 5 February 2008
Accepted for publication 27 May 2008
Published 1 September 2008
Online at stacks.iop.org/STAM/9/035004

Abstract
In this study, we investigate the antibacterial activity of ZnO nanoparticles with various particle sizes. ZnO was prepared by the base hydrolysis of zinc acetate in a 2-propanol medium and also by a precipitation method using $Zn(NO_3)_2$ and NaOH. The products were characterized by x-ray diffraction (XRD) analysis, transmission electron microscopy (TEM) and photoluminescence (PL) spectroscopy. Bacteriological tests such as minimum inhibitory concentration (MIC) and disk diffusion were performed in Luria-Bertani and nutrient agar media on solid agar plates and in liquid broth systems using different concentrations of ZnO by a standard microbial method for the first time. Our bacteriological study showed the enhanced biocidal activity of ZnO nanoparticles compared with bulk ZnO in repeated experiments. This demonstrated that the bactericidal efficacy of ZnO nanoparticles increases with decreasing particle size. It is proposed that both the abrasiveness and the surface oxygen species of ZnO nanoparticles promote the biocidal properties of ZnO nanoparticles.

Keywords: metal oxides, precipitation, transmission electron microscopy (TEM), photoluminescence, antimicrobial

1. Introduction

In recent years, ZnO being a wide band-gap semiconductor (3.36 eV), has received increased attention regarding potential electronic applications due to its unique optical, electrical and chemical properties [1]. The availability of a wide range of nanostructures makes ZnO an ideal material for nanoscale optoelectronics [2] and piezoelectric nanogenerators [3] as well as in biotechnology [4]. Furthermore, ZnO appears to strongly resist microorganisms [5]. There are some reports [6] on the considerable antibacterial activity of CaO, MgO and ZnO, which is attributed to the generation of reactive oxygen species on the surface of these oxides, studied by a conductometric method. The advantage of using these inorganic oxides as antimicrobial agents is that they contain mineral elements essential to humans and exhibit strong activity even when administered in small amounts. The activity is quantitatively evaluated by studying the growth medium caused by the bacterial metabolism. Sawai *et al* [7] examined the minimal inhibitory concentration obtained by indirect conductometric assay to evaluate the antibacterial activity of insoluble ceramic powders compared with several types of antibiotics. They reported that the activity was affected by particle size, which is controlled by processing parameters.

Many researchers have attempted to correlate the biological activity of inorganic antibacterial agents with the size of the constituent particles [8, 9]. Inorganic nanocrystalline metal oxides are particularly interesting because they can be prepared with extremely high surface areas, and are more suitable for biological applications. The advantages of inorganic antibacterial materials over organic antibacterial materials are that the former show superior durability, less toxicity and greater selectivity and heat resistance. TiO_2 and ZnO semiconductors have been extensively studied as antimicrobial agents due to their photocatalytic activity under UV light [10, 11]. Generally, the antimicrobial mechanism of chemical agents can be understood by studying the specific binding of the surface of the agent with a microorganism and the consequent

metabolism of the agents inside the microorganism. These antimicrobial substances based on inorganic chemicals have been found to be effective for therapy. In addition to oxides, many researchers have also reported the antimicrobial activity of metal ions [12, 13].

Although many studies on the biological activity of ZnO have been carried out, most of these pertain to the antimicrobial effect of bulk ZnO with a large particle size. Yamamoto [14] studied the bacterial activity of ZnO with various particle sizes in the range of 0.1–1 μm. The activity of ZnO powder slurries was measured using a conductance method. The change in electrical conductivity with bacterial growth was correlated to the antibacterial activity of ZnO, which increased with decreasing particle size. Here, we report two different methodologies for synthesizing nanosized ZnO: a precipitation method and the base hydrolysis of zinc acetate in a 2-propanol medium with a stabilizing agent. We have studied the structural and optical properties of the products and have also evaluated their biological activity by a standard microbial method adopted for metal oxides. Using both methods, it was found that the synthesized ZnO contains particles of sizes in the range of 10–50 nm. These particles exhibit both qualitatively and quantitatively better antibacterial properties than bulk ZnO with a particle size of 2 μm. The results clearly demonstrate that nanosized ZnO is a more effective antimicrobial agent than bulk ZnO. To the best of our knowledge, this is the first systematic study in which nano and bulk ZnO are compared regarding the inactivation/destruction of bacteria using a standard microbial method.

2. Experimental

2.1. Materials and methods

Zinc acetate and 2-propanol were obtained from SD-Fine Chemicals, Ltd (99% purity), 2-mercaptoethanol was obtained from Aldrich, zinc nitrate (99% purity) was obtained from Merck, and NaOH and H_2O_2 (30%) were purchased from Thomas Baker Pvt., Ltd. Double distilled water was used for all the preparations. The bacteria strain *Escherichia coli* (DH 5α) was acquired from the Biological Sciences Department, VIT University, Vellore, as well as other materials for bacterial cultivation, Pyrex petri dishes were purchased from Tarson. Phase purity and grain size were determined by x-ray diffraction (XRD) analysis recorded on a Siefert x-ray diffractometer using CuKα radiation ($\lambda = 1.54016$ Å) at 60 keV over the range of 20–70°. The average grain size was determined by x-ray line broadening using the Scherrer equation after incorporating corrections. The morphology and size of the particles were determined by high-resolution transmission electron microscopy (HRTEM) using a JEOL JEM 3010 electron microscope at an accelerating voltage of 200 keV. Samples were prepared by making a clear dispersion of the ZnO nanopowder in 2-propanol and by placing a drop of the solution on a carbon-coated copper grid. Photoluminescence (PL) spectra were recorded on a Perkin-Elmer LS 55 spectrophotometer using a xenon laser with an output power of 450 W at 300 K as the excitation source. To facilitate the measurements, the ZnO nanocrystals were compacted into pellets of 12 mm diameter and 0.4 mm thickness. The specific surface area was determined by measuring the adsorption isotherms of N_2 at −196 °C using a BET Micromeritics ASAP 2020 model.

2.2. Preparation of ZnO nanoparticles

We used two different methods for synthesizing nanocrystalline ZnO with various particle sizes. Sample 1 was synthesized by mixing zinc nitrate (0.1 M) and sodium hydroxide (0.2 M) at room temperature while constantly stirring for 2 h. The white precipitate formed was washed thoroughly with double distilled water to remove all the ions; then, centrifuged at 3000 rpm for 5 min. The procedure was repeated several times until the precipitate was free from Na^+ and NO_3^- ions. Then, 1 mol H_2O_2 was added to the precipitate to make a translucent sol maintaining temperature at 75 °C for 1 h. The obtained sol was dried in a hot air oven for 3 h and further calcined at 350 °C for 6 h to form ZnO nanocrystals.

Surface-modified nanocrystalline ZnO (sample 2) was prepared by dissolving 0.5 mmol of zinc acetate $[(CH_3COO)_2Zn \cdot 2H_2O]$ in 100 ml of 2-propanol at 80 °C while constantly stirring. To this, 0.3 mmol of 2-mercaptoethanol was added, and the mixture was continually stirred for 2 h. The 2-mercaptoethanol was introduced as a capping molecule, which stabilizes the ZnO nanoparticles. The resultant mixture was then hydrolyzed by adding 1.25 mmol of NaOH in 2-propanol followed by ultrasonic agitation for 2 h. The solvent was then removed and the product was washed with water and centrifuged at 2000 rpm. The procedure was repeated several times and then dried in an oven at 80 °C for 12 h to form ZnO nanocrystals.

2.3. Bacterial cultures and evaluation of antibacterial activities

For antibacterial experiments, *E. coli*, a Gram negative bacterium, was selected as the target organism. All disks and materials were sterilized in an autoclave before the experiments. Luria Bertani (LB) broth and nutrient agar were used as sources for culturing *E. coli* at 37 °C on a rotary platform in an incubator. The density of bacterial cells in the liquid cultures was estimated by optical density (OD) measurements at 600 nm wavelength and was maintained at 0.8–1.0, which is the ideal optical density of the cells. The cell suspensions used for antibacterial activity contained 10^5 colony-forming units (CFU) ml^{-1}. The antibacterial activity of ZnO was measured by paper disk diffusion assay in terms of minimum inhibitory concentration (MIC) and minimum bactericidal concentration (MBC).

The petri plates used in the tests were prepared using a nutrient agar medium. The bacteria were sprayed evenly on top of the plates using a sterile glass rod. After allowing the bacteria to dry (within 5–10 min) test solutions of ZnO of various concentrations (different particle sizes) were dropped within a disk of 8 mm diameter. The zone of inhibition was

measured after 18 h incubation. To evaluate the MIC, an appropriate volume of 10^5 CFU ml^{-1} *E. coli* in LB broth was added to bulk and nanosized ZnO suspensions whose concentrations varied from 0.01 to 100 mM. Compounds were tested three times and the results were averaged. Negative and positive control tubes contained only inoculated broth and free ZnO solution, respectively. The tubes were incubated at 37 °C for 18–20 h. The visual turbidity of the tubes was noted before and after incubation. Aliquots from tubes (100 μl) that appeared to have little or no cell growth were plated on nutrient agar plates to distinguish between the bacteriostatic and bactericidal effects. The plates were then incubated and the colonies were quantified.

3. Results and discussion

3.1. Preparation of nanocrystalline ZnO

There are several methods for preparing nanosized ZnO powders such as spray pyrolysis [15], precipitation [16], thermal decomposition [17], hydrothermal synthesis [18] and electrochemical growth [19]. Different methods yield different particle sizes of ZnO, depending on the type of precursor, the solvent, the pH and the temperature of the reacting solution. The choice of method depends on the final application. In this study, we employed a precipitation method to prepare nanosized ZnO, which is the easiest method for producing nanomaterials [20]. In method I, zinc nitrate and sodium hydroxide were mixed at room temperature and a precipitation reaction occurred while stirring for 2 h, after which the pH was 10.8.

$$Zn(NO_3)_2 \cdot 6H_2O + 2NaOH \longrightarrow Zn(OH)_2 + NaNO_3$$

$Zn(OH)_2$ was washed thoroughly to remove NaOH and $NaNO_3$ until the pH became neutral. Hydrogen peroxide at 75 °C was then added dropwise to produce a translucent sol of zinc peroxide, which was then heated at 350 °C to produce ZnO with active surface oxygen species.

$$Zn(OH)_2 + H_2O_2 \longrightarrow ZnO_2 \cdot 2H_2O$$

$$ZnO_2 \cdot 2H_2O \xrightarrow{\Delta} ZnO$$

In method II, zinc acetate was dissolved in 2-propanol, after which 0.3 mol thiol was added while constantly stirring. Generally, acetate-complexing ligands can form unidentate, bidentate (chelating) and bridging bonding structures with zinc ions [21]. The possible formation of $Zn_4O(Ac)_6$ is reported elsewhere [22], where the structural similarity of $Zn_4O(Ac)_6$ and ZnO, which favors the condensation of this molecular building block into ZnO, is discussed. To avoid the agglomeration, 2-mercaptoethanol was introduced as a capping agent. It has been well established that the stabilization and surface passivation of ZnO nanoparticles are vitally important for the development of their electrical and optical properties. When no capping molecules are introduced, particle interaction and aggregation are observed in ZnO sample 1 obtained by the precipitation method. The presence of capping molecules appears to affect the kinetics of nucleation and accumulation in such a way that the rate of growth of large particle decreases while that of small particles remains the same. This should result in a narrowing of the size distribution of the particles in the product.

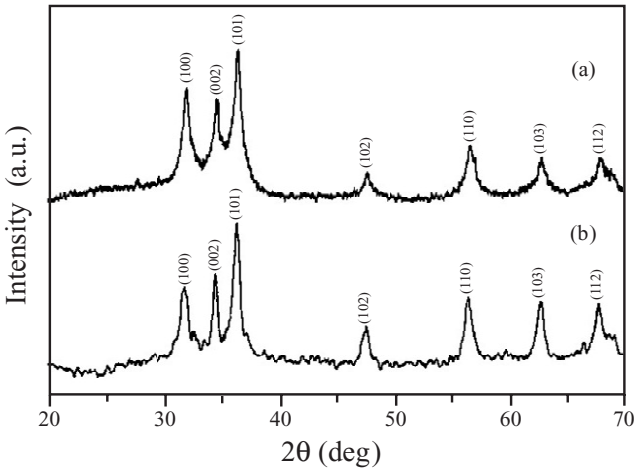

Figure 1. (a) XRD pattern of ZnO formed by precipitation method (sample 1). (b) XRD pattern of ZnO formed by base hydrolysis in propanol medium (sample 2).

3.2. Characterization of nanocrystalline ZnO

3.2.1 XRD patterns and TEM morphologies. XRD patterns of the ZnO samples prepared by the two methods are shown in figure 1. The diffraction pattern and interplanar spacing closely match those in the standard diffraction pattern of wurtzite ZnO. Figure 1(a) shows the peak broadening of the XRD pattern for sample 1. With increasing annealing temperature the crystallinity of the sample appears to improve and the grain size is also increased. The broadened peaks in the XRD pattern of sample 2 obtained by base hydrolysis (figure 1(b)) indicates the formation of ZnO nanocrystals with small crystallites. The crystallite size obtained by the two synthesis methods was estimated by the Scherrer equation and found to be in the range of 20–40 nm. Comparison of the crystallite sizes of ZnO obtained by both methods indicates that method I (precipitation) led to a higher range of crystallite size than method II (base hydrolysis of zinc acetate in propanol medium), reflecting the effect of the temperature during the process on crystallite size.

Typical TEM images of the ZnO nanoparticles are shown in figures 2(a) and (b). Direct comparison of the TEM images reveals that the uncapped ZnO nanoparticles are prone to aggregation, whereas the thiol-capped nanoparticles are well separated. The particles were found to be almost spherical. Note that ZnO nanoparticles modified by thiol have a narrow size distribution (figure 2(b)) compared with those without modification (figure 2(a)). A statistical analysis reveals that the mean particle sizes are approximately 12 nm for thiol-capped ZnO and 47 nm for ZnO without a capping agent.

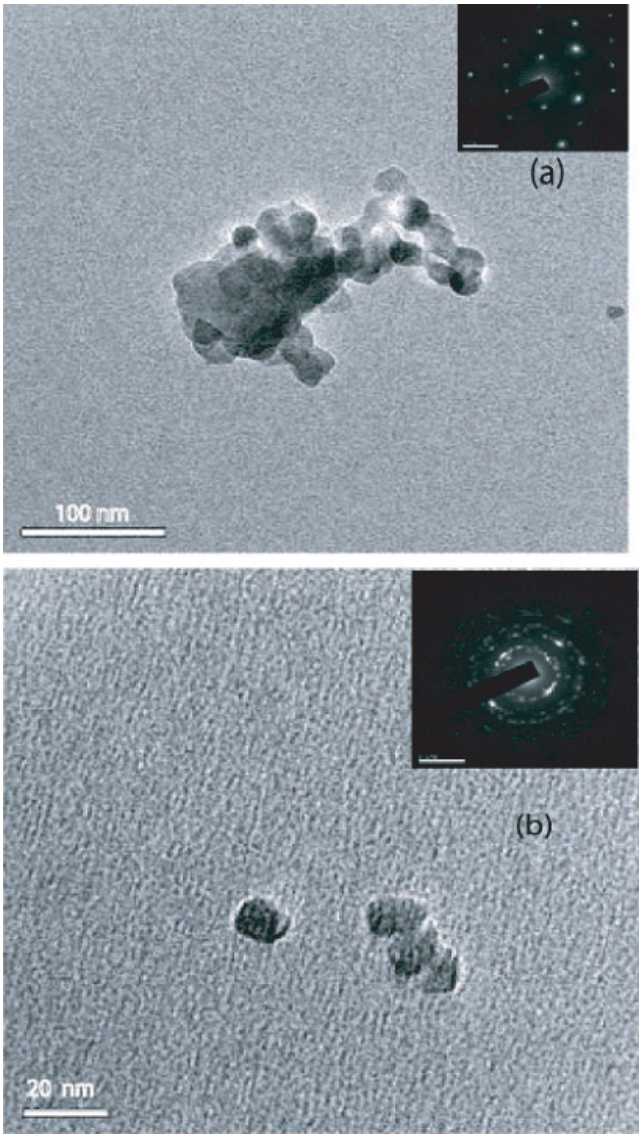

Figure 2. (a) TEM micrograph and SAED pattern (inset) of ZnO formed by precipitation method (sample 1). (b) TEM micrograph and SAED pattern (inset) of ZnO formed by base hydrolysis in propanol medium (sample 2).

It can be seen from the selected-area electron diffraction (SAED) patterns of ZnO nanocrystals that the polycrystalline diffraction spots correspond to wurtzite ZnO. In the insets of figures 2(a) and (b), the spotted diffraction rings indicate the preferential orientations of ZnO.

3.2.2 Photoluminescence. Figure 3 shows the PL spectrum of ZnO nanocrystals with an excitation wavelength at 325 nm, which is in accordance with results in the literature [23–27]. A relatively sharp, weak UV emission band at 3.23 eV (384 nm) and a broad stronger emission band in the green part of the visible spectrum with a maximum intensity at 2.4 eV (520 nm) are observed. The UV band is due to the radiative annihilation of excitons (exciton emission). The origin of the broad green emission band at 2.38 eV is attributed to surface anion vacancies [24]. It involves the tunneling of surface-bound electrons through preexisting trapped holes

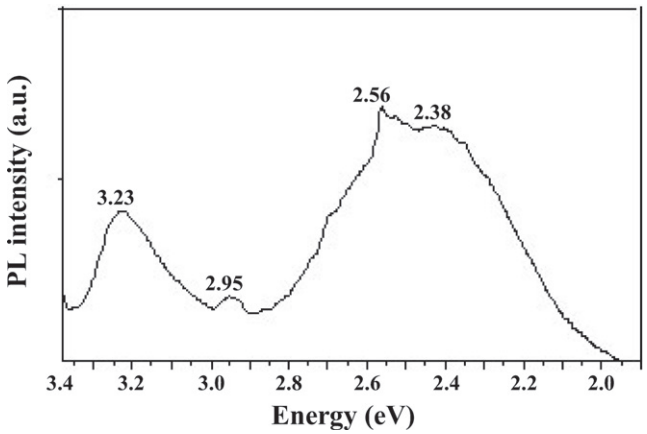

Figure 3. PL spectrum at 300 K of sample 1 synthesized by precipitation method.

Table 1. Correlation of the size of the zone of inhibition with ZnO.

ZnO particle size	Zone of inhibition (mm) *E. coli*
12 nm	31 (0.1)
45 nm	27 (0.1)
2 μm	22 (0.3)

in oxygen vacancies ($Vo^{\bullet}$) resulting in the creation of recombination centers ($Vo^{\bullet\bullet}$) for visible emission. Mo *et al* [25] elucidated this in terms of defect levels associated with oxygen vacancies and zinc interstices. These defects are most probably on the nanocrystal surfaces, causing faster and more effective trapping of the photogenerated holes at the surface sites.

The PL spectrum also exhibits two additional weak peaks at 2.95 eV (420 nm) and 2.56 eV (485 nm). These PL signals are attributed to band-edge free excitons and bound excitons, respectively [26]. The intensity of the visible emission peak also correlates with the particle size [27].

3.3. Evaluation of antibacterial properties

In our study, the relative antibacterial activity of ZnO suspensions of particles with sizes of 12 nm, 45 nm and 2 μm toward *E. coli* was studied qualitatively in aqueous LB broth by disk diffusion and quantitatively in terms of the MIC and MBC. A standard testing protocol was employed that is applicable to inorganic metal oxides and composite materials such as AgBr-polymer and Ag-SiO_2 [28, 29]. The MBC is the lowest concentration ($\mu g\,ml^{-1}$) at which a compound will kill more than 99% of the added bacteria. The MIC of the agent is the concentration at which the solution becomes turbid [30]. A lower MIC corresponds to higher antibacterial effectiveness. In terms of both MIC and MBC, we found an inverse relationship between the particle size and activity.

The ability of the antimicrobial agent to rupture bacterial cells is tested by the disk diffusion method. Here, three ZnO suspensions with different particle sizes were tested, and the results are given in table 1. The presence of an inhibition zone clearly indicates that the mechanism of the biocidal action

Table 2. Comparison of biocidal effect of micron and nano ZnO by MIC towards *E. coli*.

Sample (ZnO)	MIC (μg ml^{-1})	Status of bioactivity (after 24 hr incubation)
0.01 mM	0.8	lawn
0.1 mM	8	lawn
1 mM	80	bacteriostatic
5 mM	400	bactericidal
10 mM	800	bactericidal
50 mM	4000	bactericidal
100 mM	8000	bactericidal

of ZnO involves disrupting the membrane. The high rate of generation of surface oxygen species from ZnO leads to the death of the bacteria. Interestingly, the size of the inhibition zone increased significantly with decreasing size of the ZnO particles.

MIC and MBC were determined by the standard microbial method. ZnO suspensions with different concentrations of micron-sized and nanosized ZnO were incubated with *E. coli* in aqueous LB broth. Bacterial growth was studied by visually inspecting the LB broth for turbidity. If the material being tested does not kill but instead inhibits the growth of bacteria (bacteriostatic agent), the bacteria will grow when it is removed from the solution containing the material, and colonies will be observed upon plating an aliquot. If the material being tested is bactericidal, the absence of bacterial colonies will be observed upon plating. To establish whether the suspensions were bacteriostatic or bactericidal, 100 μl aliquots were taken from the incubated LB broth, each containing ZnO and *E. coli*, and were plated on nutrient agar plates and incubated for 18–20 h. The results are summarized in table 2. ZnO suspension with a concentration in the range of 100 to 5 mM effectively inhibits bacterial growth. No significant antibacterial activity was observed at concentrations less than 1 mM for all the ZnO samples. However, the bactericidal efficacy at 1 mM is higher for the 12 nm ZnO suspension (sample 2–86%) than for the 45 nm and 2 μm ZnO suspensions.

The bactericidal efficacies of ZnO suspensions with three different particle sizes after 24 h incubation of the aliquots are shown in figures 4(a) and (b) in the lowest concentration range (0.01–1 mM) and the highest concentration range (5–100 mM), respectively. We noticed that in both cases, the ZnO suspension with 12 nm particles is more effective than the suspensions with other particle sizes. This can be explained on the basis of the oxygen species released on the surface of ZnO, which cause fatal damage to microorganisms [31]. The generation of highly reactive species such as OH^-, H_2O_2 and O_2^{2-} is explained as follows. Since ZnO with defects can be activated by both UV and visible light, electron-hole pairs (e^-h^+) can be created. The holes split H_2O molecules (from the suspension of ZnO) into OH^- and H^+. Dissolved oxygen molecules are transformed to superoxide radical anions ($^\bullet O_2^-$), which in turn react with H^+ to generate ($HO_2^\bullet$) radicals, which upon subsequent collision with electrons produce hydrogen peroxide anions (HO_2^-). They then react with hydrogen ions to produce molecules of

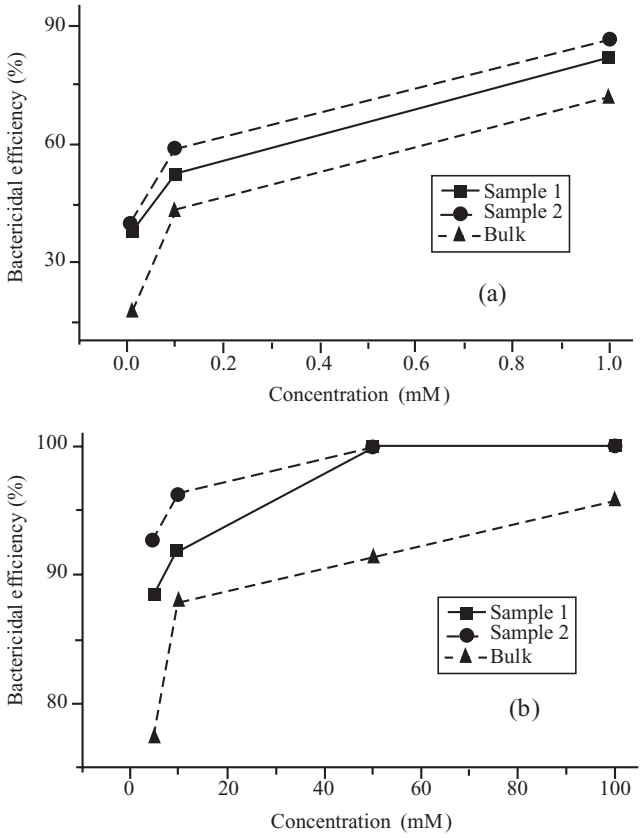

Figure 4. (a) and (b) Bactericidal efficiency of sample 1, 2 and bulk ZnO suspensions at different concentrations.

H_2O_2. The generated H_2O_2 can penetrate the cell membrane and kill the bacteria [32].

$$ZnO + h\nu \rightarrow e^- + h^+;\ h^+ + H_2O \rightarrow {}^\bullet OH + H^+.$$

$$e^- + O_2 \rightarrow {}^\bullet O_2^-;\quad {}^\bullet O_2 + H^+ \rightarrow HO_2^\bullet$$

$$HO_2^\bullet + H^+ + e^- \rightarrow H_2O_2$$

Since, the hydroxyl radicals and superoxides are negatively charged particles, they cannot penetrate into the cell membrane and must remain in direct contact with the outer surface of the bacteria; however, H_2O_2 can penetrate into the cell [33].

Considering the size of the bacteria, it is evident that a single isolated colony of *E. coli* of 2 μm diameter can accommodate a large number of 12 nm particles of ZnO (sample 2) and fewer 45 nm particles (sample 1), resulting in different biocidal properties of the two suspensions. Once ZnO kills/captures the cell membrane, the ZnO nanoparticles presumably remain tightly adsorbed on the surface of the leftover/dead bacteria preventing further antibacterial action. However, ZnO nanoparticles continue to release peroxides into the medium even after the surface of the dead bacteria are completely covered by ZnO nanoparticles, thereby showing high bactericidal efficacy. From the results for MIC, we confirm that the smaller particle size shows enhanced activity due to the large surface area to volume ratio and the surface

reactivity of ZnO. In comparison, the bulk ZnO showed less bactericidal activity than ZnO nanoparticles. From the BET measurement, the specific surface area of sample 1 (mean particle size is 47 nm by TEM) is found to be 68 $m^2\,g^{-1}$, whereas that of sample 2 (mean particle size is 12 nm by TEM) is 115 $m^2\,g^{-1}$. The agglomeration of ZnO nanoparticles is minimized by the presence of the capping agent (2-mercaptoethanol) in sample 2. ZnO nanoparticles of both sizes have a high surface area compared with bulk ZnO (5.11 $m^2\,g^{-1}$). The generation of H_2O_2 depends strongly on the surface area of ZnO, which results in more oxygen species on the surface and the higher antibacterial activity of the smaller nanoparticles [34].

The detailed mechanism for the activity of ZnO is still under debate. One possible explanation of the antibacterial effect of ZnO is based on the abrasive surface texture of ZnO. ZnO nanoparticles have been found to be abrasive due to surface defects [9]. The PL spectrum of ZnO (figure 3) confirms the presence of surface defects (broad visible emission band) in the region of 450–550 nm. The abrasiveness of ZnO nanoparticles compared with bulk ZnO is caused by the uneven surface texture due to rough edges and corners. This surface roughness contributes to the mechanical damage of the cell membrane of *E. coli*. Wang *et al* [35] proposed that the orientation of ZnO can also affect bioactivity. They showed that randomly oriented ZnO nanowires show higher antibacterial activity than regularly oriented ZnO nanowires due to the different spatial arrangements of ZnO causing the biocidal activity. The interaction of metal ions including zinc with microbes has also been studied [36].

ZnO suspensions in the lower concentration range (0.01–1 mM) seem to exhibit less antimicrobial activity. This may be due to the possible presence of fewer Zn^{2+} ions, which might act as nutrient [37]. To verify this, we studied the antimicrobial activity of $ZnCl_2$ with different concentrations (in suspensions similar to those of ZnO at various pH values). The initial pH of 5 mM $ZnCl_2$ suspensionwas 5.9 (weakly acidic), which resulted in the rapid bacterial growth of *E. coli*, indicating that Zn^{2+} is not toxic at lower concentrations and at this pH. The reason for this may be that zinc is an essential cofactor in a variety of cellular processes. Although metals and metal oxides are known to be toxic at relatively high concentrations, they are not expected to be toxic at low concentrations. To investigate the survival of bacteria under acidic conditions the pH was lowered by adding acetic acid (0.1 M) dropwise and the pH was maintained at 2.3. As anticipated, no colonies were seen on the plate. We then increased the pH by adding 0.1 M NaOH dropwise until it reached 8.5 (weakly basic). No colonies were observed at this pH. This indicates that a pH in the range of 6–8 does not affect the growth of the bacteria, irrespective of the metal ions present. We could only observe a bacteriostatic effect above a $ZnCl_2$ concentration of 20 mM. Excess metal ions are toxic to bacterial cells. Therefore, some bacteria have developed mechanisms to regulate the influx and efflux processes to maintain a steady intracellular concentration of ions including Zn^{2+} ions [38]. In this study we demonstrated the formation of large numbers of colonies (a bacterial lawn) when the MIC is less than 1 mM, illustrating the known fact that Zn^{2+} ions are a supplement promoting the metabolic action of bacteria at trace concentrations.

We have studied the antimicrobial activity of ZnO powders with particle sizes ranging from microns to nanometers and found that ZnO nanoparticles show greater inhibition than microcrystalline ZnO according to the results of tests by a standard microbial method. It can be concluded that the cell wall rupture must be due to the surface activity of ZnO in contact with the bacteria. It is believed that cell death is caused by the decomposition of the cell wall followed by the subsequent decomposition of the cell membrane. The damage to the cell membrane directly leads to the leakage of minerals, proteins and genetic materials, causing cell death. The results of this study may be applicable to medical devices that are coated with nanoparticles against microbes.

4. Conclusion

We have demonstrated the enhanced bioactivity of ZnO nanoparticles by studying the antimicrobial activity of suspensions with various particle sizes using a standard microbial method for the first time. The enhanced bioactivity of smaller particles is attributed to the higher surface area to volume ratio. For smaller ZnO nanoparticles, more particles are needed to cover a bacterial colony (2 μm) which results in the generation of a larger number of active oxygen species (released from ZnO on the surface of the colony), which kill bacteria more effectively. ZnO nanoparticles were found to be more abrasive than bulk ZnO, and thus contribute to the greater mechanical damage of the cell membrane and the enhanced bactericidal effect of ZnO nanoparticles.

Acknowledgments

The authors thank the VIT management and the DRDO Grant in aid scheme, Government of India, for financial assistance. The authors thank Dr A Radha for her help in antimicrobial study and Professor T Pradeep, IITM, for his help in TEM imaging.

References

[1] Baxter J B and Aydil E S 2005 *Appl. Phys. Lett.* **86** 53114
[2] Huang M H, Mao S, Feick H, Yan H Q, Wu Y, Kind H, Weber E, Russo R and Yang P 2001 *Science* **292** 1897
[3] Song J, Zhou J and Wang Z L 2006 *Nano Lett.* **6** 1656
[4] Wang Z L 2004 *Annu. Rev. Phys. Chem.* **55** 159
[5] Sawai J, Igarashi H, Hashimoto A, Kokugan T and Shimizu M 1996 *J. Chem. Eng. Japan* **29** 556
[6] Sawai J and Yoshikawa T J 2004 *Appl. Microbiol.* **96** 803
[7] Sawai J, Doi R, Maekawa Y, Yoshikawa T and Kojima H 2002 *J. Ind. Microbiol. Biotech.* **29** 296
[8] Brayner R, Ferrari-Iliou R, Brivois N, Djediat S, Benedetti M F and Fievet F 2006 *Nano Lett.* **6** 866
[9] Stoimenov P K, Klinger R L, Marchin G L and Klabunde K J 2002 *Langmuir* **18** 6679
[10] Fortuny A, Bengoa C, Font J and Fabregat A 1999 *J. Hazard Mater.* **64** 181
[11] Rana S, Rawat J, Sorensson M M and Misra R D K 2006 *Acta Biomater.* **2** 421

[12] Russell A D and Hugo W B 1994 *Prog. Med. Chem.* **31** 351
[13] Shanmugam S, Viswanathan B and Varadarajan T K 2006 *Mater. Chem. Phys.* **95** 51
[14] Yamamoto O 2001 *Int. J. Inorg. Mater.* **3** 643
[15] Liu T Q, Sakurai O, Mizutani N and Kato M 1986 *J. Mater. Sci.* **21** 3698
[16] Trindade T, Pedrosa Jesus J D and O'Brien P 1994 *J. Mater. Chem.* **4** 1611
[17] Verges M A and Gallego M M 1992 *J. Mater. Sci.* **27** 3756
[18] Chen D, Jiao X and Cheng G 2000 *Solid State Commun.* **113** 363
[19] Mahamuni S, Borgohain K, Bendre B S, Valene J L and Subhash H R 1999 *J. Appl. Phys.* **85** 2861
[20] Wang Y, Ma C, Sun X and Li H 2002 *Inorg. Chem. Commun.* **5** 751
[21] Sakohara S, Ishida M and Anderson M A 1998 *J. Phys. Chem.* B **102** 10169
[22] Tokumoto M S, Briois V, Santilli C V and Pulcinelli S H 2003 *J. Sol-Gel Sci. Technol.* **26** 547
[23] Dijken A V, Meulenkamp E A, Vanmaekelbergh D and Meijerink A 2000 *J. Lumin.* **87** 454
[24] Du Y, Zhang M S, Hong J, Shen Y, Chen Q and Yin Z 2003 *Appl. Phys.* A **76** 171
[25] Mo C M, Li Y H, Lin Y S, Zhang Y and Zhang P L 1998 *J. Appl. Phys.* **83** 4389
[26] Liqianga J, Yichuna Q, Baiqia W, Shudana L, Baojianga J, Libina Y, Weia F, Honggang F and Jiazhong S 2006 *Sol. Energy Mater. Sol. Cells* **90** 1773
[27] Wang M, Na E K, Kim J S, Kim E J, Hahn S H, Park C and Koo K K 2007 *Mater. Lett.* **61** 4094
[28] Sambhy V, MacBride M M, Peterson B R and Sen A 2006 *J. Am. Chem. Soc.* **128** 9798
[29] Wang J X, Wen L X, Wang Z H and Chen J F 2006 *Mater. Chem. Phys.* **96** 90
[30] Tortora G, Funke R B and Case L C 2001 *Microbiology—An Introduction* (New York: Longman)
[31] Sunada K, Kikuchi Y, Hashimoto K and Fujshima A 1998 *Environ. Sci. Technol.* **32** 726
[32] Fang M, Chen J H, Xu X L, Yang P H and Hildebrand H F 2006 *Int. J. Antimicrob. Agents* **27** 513
[33] Blake M D, Maness P, Huang Z, Wolfrum E J, Huang J and Jacoby W A 1999 *Sep. Purif. Methods* **28** 1
[34] Yamamoto O, Komatsu M, Sawai J and Nakagawa Z 2008 *J. Mater. Sci. Mater. Med.* **19** 1407
[35] Wang X, Yang F, Yang W and Yang X 2007 *Chem. Commun.* **42** 4419
[36] Amro N A, Kotra L P, Mesthrige K W, Bulychev A, Mobashery S and Liu G 2000 *Langmuir* **16** 2789
[37] Sawai J 2003 *J. Microbiol. Methods* **54** 177
[38] Gaballa A and Helmann J P 1998 *J. Bacteriol.* **180** 5815